Pericyte–fibroblast transition promotes tumor growth and metastasis

Kayoko Hosaka[a], Yunlong Yang[a,b], Takahiro Seki[a], Carina Fischer[a], Olivier Dubey[a], Erik Fredlund[c], Johan Hartman[c], Piotr Religa[d], Hiromasa Morikawa[e], Yoko Ishii[f], Masakiyo Sasahara[f], Ola Larsson[c], Giulio Cossu[g], Renhai Cao[a], Sharon Lim[a], and Yihai Cao[a,b,h,1]

[a]Department of Microbiology, Tumor and Cell Biology, Karolinska Institute, 171 77 Stockholm, Sweden; [b]Key Laboratory of International Collaborations, Second People's Hospital of Shenzhen, First Affiliated Hospital of Shenzhen University, Shenzhen 518035, China; [c]Department of Oncology-Pathology, Karolinska Institute, 171 77 Stockholm, Sweden; [d]Center for Molecular Medicine, Department of Medicine, Solna, Karolinska Institute, 171 76 Stockholm, Sweden; [e]Unit of Computational Medicine, Department of Medicine, Center for Molecular Medicine, Karolinska Institute, 171 76 Stockholm, Sweden; [f]Department of Pathology, Graduate School of Medicine and Pharmaceutical Sciences, University of Toyama, Toyama 930-0194, Japan; [g]Department of Cell and Developmental Biology, University College London, London WC1E 6DE, United Kingdom; and [h]Department of Cardiovascular Sciences, University of Leicester and National Institute for Health Research Leicester Cardiovascular Biomedical Research Unit, Glenfield Hospital, Leicester LE1 7RH, United Kingdom

Edited by Tadamitsu Kishimoto, Osaka University, Suita, Japan, and approved July 26, 2016 (received for review May 25, 2016)

Vascular pericytes, an important cellular component in the tumor microenvironment, are often associated with tumor vasculatures, and their functions in cancer invasion and metastasis are poorly understood. Here we show that PDGF-BB induces pericyte–fibroblast transition (PFT), which significantly contributes to tumor invasion and metastasis. Gain- and loss-of-function experiments demonstrate that PDGF-BB-PDGFRβ signaling promotes PFT both in vitro and in in vivo tumors. Genome-wide expression analysis indicates that PDGF-BB–activated pericytes acquire mesenchymal progenitor features. Pharmacological inhibition and genetic deletion of PDGFRβ ablate the PDGF-BB–induced PFT. Genetic tracing of pericytes with two independent mouse strains, *TN-AP-CreERT2:R26R-tdTomato* and *NG2-CreERT2:R26R-tdTomato*, shows that PFT cells gain stromal fibroblast and myofibroblast markers in tumors. Importantly, coimplantation of PFT cells with less-invasive tumor cells in mice markedly promotes tumor dissemination and invasion, leading to an increased number of circulating tumor cells and metastasis. Our findings reveal a mechanism of vascular pericytes in PDGF-BB–promoted cancer invasion and metastasis by inducing PFT, and thus targeting PFT may offer a new treatment option of cancer metastasis.

pericyte | PDGF | fibroblast | metastasis | mesenchymal cell

The tumor microenvironment possesses diverse cellular components including malignant cells, inflammatory cells, stromal fibroblasts, various progenitor cells, endothelial cells, and perivascular cells. These tumor-associated cellular components constantly change their identities and functions to cope with tumor growth and invasiveness (1). Tumor cells often produce various growth factors and cytokines as instrumental signals to manipulate host cells that in most cases facilitate tumor growth and metastasis. Although the role of endothelial, inflammatory, and mesenchymal cells in tumor growth and invasion have been extensively studied (2–10), functions of pericytes in the tumor microenvironment remain largely unknown.

Pericytes are mainly described as mural cells that are associated with vasculatures in various healthy and pathological tissues (11). Recruitment of pericytes to newly formed angiogenic vessels prevents excessive sprouting, stabilizes the nascent vasculature, prevents vascular leakiness, and remodels primitive vasculatures toward mature vasculatures (12, 13). It is believed that these vasculature-related pericyte functions could possibly impede tumor invasion and metastasis. Recent studies show that pericytes retain progenitor cell properties and can differentiate into other cells, including adipocytes, chondrocytes, osteoblasts, phagocytes, granulocytes, and skeletal muscle (14–18). Under pathological conditions, pericytes may differentiate into myofibroblasts, contributing to kidney fibrosis (19, 20). Unlike most host cells in tumors, pericytes exhibit unique features by expressing a number of surface markers and respond to certain growth factors. The PDGF-BB-PDGFRβ signaling pathway is best known for its modulation of pericyte coverage on microvessels, and endothelial cells are the primary source of PDGF-BB (11). Endothelial cell-derived PDGF-BB recruits pericytes onto angiogenic vessels through activation of PDGFRβ. Deletion of *Pdgfb* or *Pdgfrβ* genes in mice resulted in vascular defect-related embryonic lethality due to lack of pericytes (21, 22), indicating the pivotal role of PDGF-BB-PDGFRβ signaling in pericyte biology. Various tumors also express a high level of PDGF-BB and the impact of tumor cell-derived PDGF-BB on pericytes is controversial. In contrast to endothelial cells, tumor cell-derived PDGF-BB may potentially attract pericytes to migrate from vessels through a chemoattractant gradient mechanism (23). The fate of vessel disassociated pericyte (PC) has not been clearly investigated. PDGF receptor signaling has been suggested to contribute to pericyte–myofibrolast transition in kidney fibrosis (19).

CAFs, especially myofibroblasts, are known to facilitate tumor invasion and metastasis (6). In certain tumor types such as pancreatic cancers, CAFs dominate tumor cellular components and constitute a major part of the tumor mass (24). Unresolved key issues include the origin of CAFs and the signaling pathways that control the CAF population in tumor tissues. Could it be

Significance

We show that vascular pericytes significantly contribute to cancer invasion and metastasis by the mechanism of the pericyte–fibroblast transition (PFT). This study proposes this concept and indicates the vascular pericyte's role. Vascular pericytes were considered to remodel tumor vessels toward a mature phenotype. However, once dissociated from tumor vessels their functions within the tumor tissue are not known. In the present study, we show that pericytes, once detached from tumor microvasculatures, underwent differentiation to become stromal fibroblasts, which are known to contribute to tumor invasion and metastasis. Our results show that vascular pericytes are the important source of stromal fibroblasts and targeting PFT may offer a new treatment option in cancer metastasis.

Author contributions: K.H. and Y.C. designed research; K.H., Y.Y., T.S., C.F., O.D., E.F., P.R., H.M., Y.I., O.L., R.C., and S.L. performed research; J.H., M.S., and G.C. contributed new reagents/analytic tools; E.F., H.M., and O.L. analyzed microarray data; J.H. and P.R. provided clinical samples; M.S. and G.C. provided genetic mice; K.H. and Y.C. analyzed data; and Y.C. wrote the paper.

The authors declare no conflict of interest.

This article is a PNAS Direct Submission.

Data deposition: The sequences reported in this paper have been deposited in the Gene Expression Omnibus (GEO) database, www.ncbi.nlm.nih.gov/geo (accession nos. GSE85955 and GSE33717).

[1]To whom correspondence should be addressed. Email: yihai.cao@ki.se.

This article contains supporting information online at www.pnas.org/lookup/suppl/doi:10.1073/pnas.1608384113/-/DCSupplemental.

possible that other host cells in tumors differentiate into CAFs under the influence of specific signaling systems? In the present study, we provide evidence to demonstrate that vascular pericytes are an important source of CAFs, which markedly promote cancer metastasis. The pericyte–CAF transition is modulated by PDGF-BB-PDGFRβ signaling through the mechanism of pericyte–fibroblast transition (PFT). Gain- and loss-of-function experiments using genetic and pharmacological approaches validate that PFT in tumors is the primary driving force for cancer invasion and metastasis. Genetic tracing in tumor-bearing mice demonstrates that a significant number of pericytes undergo PFT. Finally, we provide evidence that PDGF-BB expression levels and fibroblast components correlate with poor survival in patients with different cancer types. Thus, our findings are clinically relevant and shed mechanistic insights on pericyte-mediated cancer metastasis and suggest that targeting PFT may potentially offer a new therapeutic option for cancer treatment.

Results

PDGF-BB Expression and Stromal Fibroblast Components in Naturally Occurring Human Tumors. To study the role of PDGF-BB, the pluripotent member of the PDGF family, in supporting CAFs, we analyzed expression levels of PDGF-BB mRNA and protein in a dozen human tumor cell lines. We previously reported a high PDGF-BB expression level in SC-A431 squamous carcinoma tumor tissue and a low PDGF-BB expression level in NB-IMR32 neuroblastoma tumor tissue (23). We have now validated those in vivo findings with in vitro cell cultures. Naturally occurring SC-A431 squamous carcinoma cells expressed a high level of PDGF-BB (40 pg/mL) in a 48-h-conditioned medium (Fig. 1*A*). In contrast, a renal cell carcinoma (RCC-CAKI-1) and a neuroblastoma (NB-IMR32) have undetectable levels of PDGF-BB.

Immunohistochemical staining of tumor tissues showed that these tumors contained high densities of microvessels and

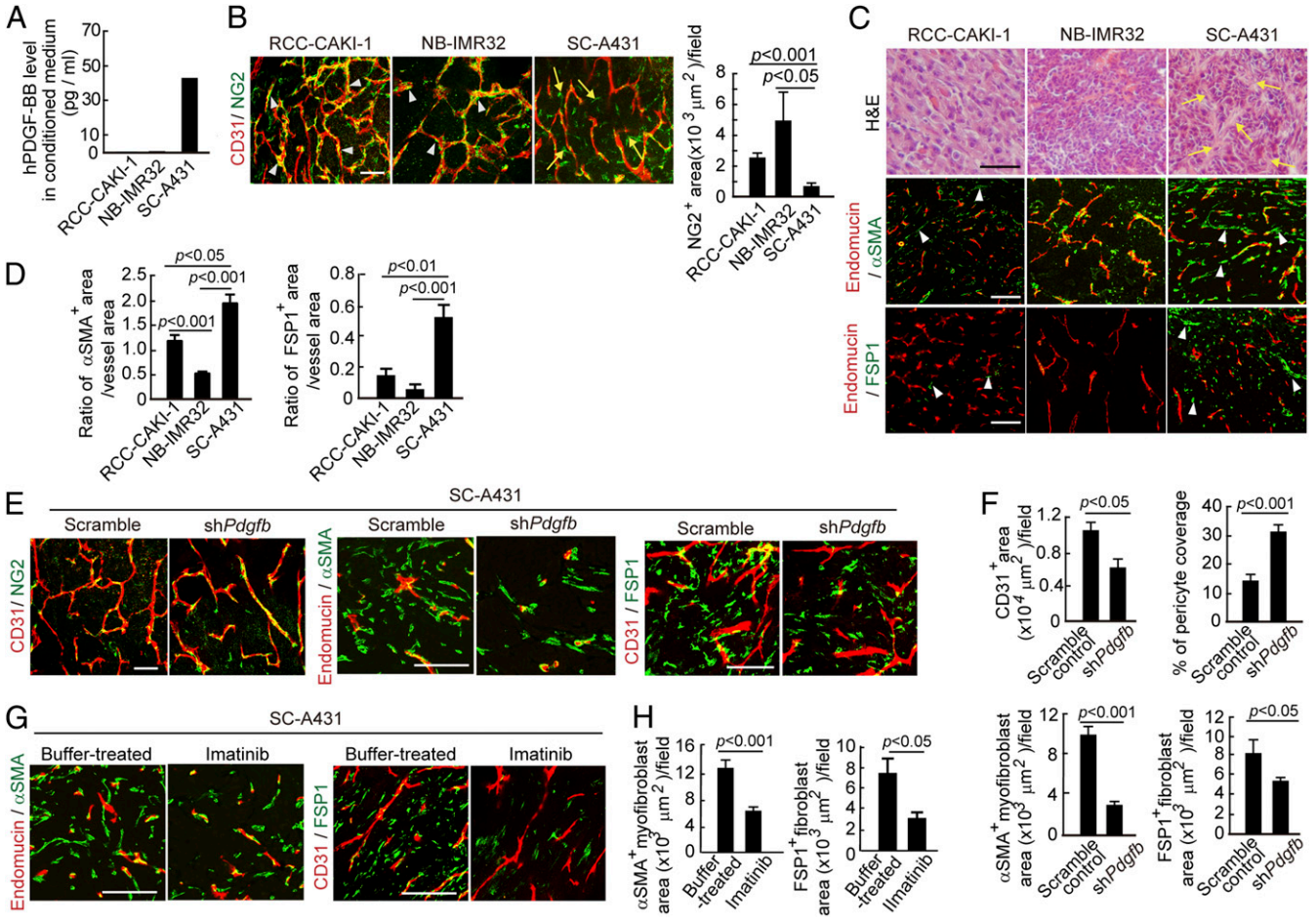

Fig. 1. Knockdown of PDGF-BB expression and inhibition of PDGFR signaling decrease stromal fibroblasts. (*A*) Expression levels of PDGF-BB protein in RCC-CAKI-1, NB-IMR32, and SC-A431 tumor cells in conditioned medium. (*B*) Tumor microvessels and stromal components. CD31$^+$ (red) endothelial cell and NG2$^+$ pericyte signals (green) in various tumors. Arrowheads point to vessel-associated pericytes; arrows indicate vessel-disassociated pericytes. Quantification of NG2$^+$ pericyte area (n = 7 random fields per group). (Scale bar, 50 μm.) (*C*, *Top*) H&E staining of tumor tissues. Arrows point to tumor stroma. (Scale bar, 100 μm.) (*Middle*) Endomucin$^+$ tumor vessels (red) and αSMA$^+$ cells (green). Arrowheads point to αSMA$^+$ myofibroblasts. (Scale bar, 100 μm.) (*Bottom*) Endomucin$^+$ tumor vessels (red) and FSP1$^+$ stromal fibroblasts (green). Arrowheads point to stromal fibroblasts. n = 4 animals per group. (Scale bar, 100 μm.) (*D*) Quantification of the ratio of αSMA$^+$ signals vs. microvascular areas (n = 12 random fields per group) and the ratio of FSP1$^+$ signals vs. microvascular areas (n = 12 random fields per group) in various human tumors. (*E*) CD31$^+$ (red) endothelial cell and NG2$^+$ pericyte signals (green), endomucin$^+$ tumor vessels (red) and αSMA$^+$ cells (green), and CD31$^+$ tumor vessels (red) and FSP1$^+$ stromal fibroblasts (green) in scrambled-shRNA and *Pdgfb*-shRNA–transfected SC-A431tumors. (Scale bars: left panels, 50 μm; middle and right panels, 100 μm.) (*F*) Quantification of microvessel density (n = 7 random fields per group), pericyte coverage (n = 7 random fields per group), αSMA$^+$ myofibroblast signals (n = 12 random fields per group), and FSP1$^+$ signals (n = 12 random fields per group) in scrambled-shRNA and *Pdgfb*-shRNA–transfected SC-A431tumors. (*G*) Endomucin$^+$ tumor vessels (red) and αSMA$^+$ cells (green) and CD31$^+$ tumor vessels (red) and FSP1$^+$ stromal fibroblasts (green) in imatinib- and buffer-treated SC-A431tumors. (Scale bar, 100 μm.) (*H*) Quantification of αSMA$^+$ myofibroblast signals (n = 12 fields per group) and FSP1$^+$ signals (n = 12 random fields per group) in imatinib- and buffer-treated SC-A431tumors. Data are represented as mean ± SEM.

decreased $NG2^+$ pericyte area (Fig. 1*B*) (23). SC-A431 tumors possessed high content of fibroblast-specific protein 1 $(FSP1)^+$ stromal fibroblast and α-smooth muscle actin $(\alpha SMA)^+$ myofibroblast components (Fig. 1 *C* and *D*). To exclude the possibility that αSMA^+ cell populations were vascular smooth muscle cells (VSMCs), tumor tissues were costained with αSMA and endomucin (a pan-endothelial cell specific marker). Notably, the majority of αSMA^+ cell populations did not show association with endomucin$^+$ positive signals (Fig. 1*C*), suggesting that the majority of αSMA^+ cells were myofibroblasts but not VSMCs. In contrast to SC-A431, both RCC-CAKI-1 and NB-IMR32 tumors have much fewer $FSP1^+$ and αSMA^+ fibroblast components. These findings suggest a possible link between PDGF-BB expression and high content of CAFs in naturally occurring human tumors.

Genetic Knockdown and Pharmacological Inhibition of the PDGF-BB-PDGFR Signaling Ablates CAFs in Human Tumors. To investigate the relation between PDGF-BB expression and the stromal CAF composition in SC-A431 tumors, *Pdgfb* mRNA was knocked down using a specific shRNA. This approach effectively ablated the expression level of *Pdgfb* (Fig. S1*A*). Knockdown of *Pdgfb* significantly increased pericyte coverage in tumor microvessels (Fig. 1 *E* and *F*). Conversely, $FSP1^+$ and αSMA^+ stromal fibroblasts and myofibrolasts were markedly decreased in *Pdgfb*-shRNA–transfected compared with scrambled-shRNA–transfected SC-A431 tumors (Fig. 1 *E* and *F*).

To further validate these findings, SC-A431 tumors were treated with imatinib, a BCL-ABL tyrosine kinase inhibitor with a potential inhibitory effect on the PDGFR signaling (25–27). Imatinib inhibited SC-A431 tumor growth and the tumor growth of other cell lines as previously described (23, 28). Similar to the shRNA knockdown approach, imatinib treatment also restored pericyte coverage in tumor microvessels as previously described (23). Importantly, treatment with imatinib markedly reduced the stromal $FSP1^+$ fibroblast and αSMA^+ myofibroblast components in tumors (Fig. 1 *G* and *H*). These data demonstrate that the PDGF-BB-PDGFR signaling significantly contributes to increases of CAFs in naturally occurring human tumors.

Gain of Function of PDGF-BB in Mouse Tumors Enhances CAFs and Decreases Pericytes. To further validate our findings in naturally occurring human tumors, we next performed a gain-of-function experiment by overexpressing PDGF-BB in mouse tumors that lacked detectable PDGF-BB as previously described (23). Similar to human SC-A431 tumors, overexpression of PDGF-BB in T241 fibrosarcoma and Lewis lung carcinoma (LLC) nearly completely ablated pericytes in tumors as previously described (23). Both vessel- and nonvessel-associated pericytes were depleted by overexpression of PDGF-BB (23). The decrease in pericytes in PDGF-BB–expressing T241 and LLC tumors was not due to pericyte apoptosis, because the pericyte apoptotic rates in $PDGF\text{-}BB^+$ and $PDGF\text{-}BB^-$ tumors were similar (Fig. S2*A*). Expression of PDGF-BB in T241 and LLC tumors led to a marked increase of $FSP1^+$ stromal fibroblasts and αSMA^+ myofibrolasts, which were disassociated with tumor microvasculatures (Fig. S2 *B*–*E*). Consequently, total amounts of stromal components in these PDGF-BB–expressing tumors were markedly increased relative to PDGF-BB–negative tumors (Fig. S2*F*). These gain-of-function experiments provide independent evidence that PDGF-BB is primarily responsible for recruitment of CAFs and cancer-associated myofibroblasts (CAMFs).

Additionally, PDGFRβ blockade treatment markedly decreased the populations of $FSP1^+$ stromal fibroblasts and αSMA^+ myofibrolasts in tumors (Fig. S2 *G* and *H*). In contrast to PDGFRβ blockade, anti-PDGFRα treatment did not significantly alter the $FSP1^+$ and αSMA^+ stromal fibroblast components in PDGF-BB–expressing tumors (Fig. S3 *A* and *B*), suggesting that PDGF-BB-PDGFRα signaling is not significantly involved in mediating the PDGF-BB–induced expansion of stromal fibroblasts. Similar to PDGFRβ blockade, treatment of T241-PDGF-BB tumors with imatinib resulted in nearly identical effects of pericyte restoration and loss of CAFs and CAMFs (Fig. S2 *G* and *H*). Also, treatment with an anti-PDGFRα neutralizing antibody increased $NG2^+$ signals that were disassociated with blood vessels (Fig. S3 *C* and *D*). In addition to alterations of pericytes and stromal fibroblasts, treatment using imatinib, but not anti-PDGFRα, significantly inhibited tumor angiogenesis (20). Both anti-PDGFRβ and imatinib treatments significantly inhibited the growth rates of T241-PDGF-BB tumors as previously described (23). In contrast, treatment using anti-PDGFRα antibody did not alter the tumor growth rate significantly (Fig. S3*E*). To further validate our findings, we treated the established tumors (tumor size around 0.4 cm^3) with PDGFRβ blockade and imatinib and obtained nearly identical results of fibroblast loss, reduction of stromal components, and inhibition of the tumor growth rate (Fig. S4). These gain-of-function results from mouse models validate our findings in human tumor models that the PDGFRβ-mediated signaling pathway is critical for the expansion of CAFs and CAMFs in tumors.

Genetic Deletion of PDGFRβ in Mice Attenuates PDGF-BB–Recruited Stromal Fibroblasts and Myofibrolasts. To further define the receptor signaling pathways that mediate PDGF-BB–recruited CAFs and CAMFs, we genetically deleted PDGFRβ in mice in a conditional knockout model (29, 30). Deletion of PDGFRβ significantly decreased vascular pericyte coverage in PDGF-BB–negative control vector tumors, supporting the vascular function of PDGF-BB in recruitment of pericytes to angiogenic vessels (Fig. S5 *A* and *B*). In contrast, implantation of PDGF-BB tumors in $Pdgfr\beta^{-/-}$ mice resulted in increased pericyte coverage on tumor vessels, as seen with the PDGFRβ blockade. It is possible that PDGFRα also played a role in recruitment of pericytes in this experimental setting. The $CD31^+$ microvessel density in vector and PDGF-BB tumors was also decreased in $Pdgfr\beta^{-/-}$ mice (Fig. S5 *A* and *B*). Similar to pharmacological approaches, genetic deletion of $Pdgfr\beta^{-/-}$ significantly decreased $FSP1^+$ CAF and αSMA^+ CAMF components in tumors (Fig. S5 *C* and *D*). These results obtained from genetic defective models provide independent evidence to support the crucial role of PDGF-BB-PDGFRβ signaling in recruitment of CAFs and CAMFs.

PDGF-BB Promotes PFT of Isolated Mouse Pericytes. The loss of $NG2^+$ pericytes and increase of CAFs and CAMFs in PDGF-BB–expressing tumors suggested that vascular pericytes might undergo differentiation into stromal fibroblasts. To investigate this possibility, we isolated primary pericytes and stimulated them with PDGF-BB in vitro for an extended period. First, we observed that PDGF-BB–stimulated pericytes changed their morphologies to an elongated and spindle-like cell shape that was morphologically similar to that of fibroblasts (Fig. 2 *A* and *B*), and PDGF-BB had no effect on pericyte apoptosis compared with vehicle-stimulated controls (Fig. S6 *A* and *B*). After 5-d stimulation with PDGF-BB, pericytes lost their NG2 expression (Fig. 2 *A* and *B*). Surprisingly, the PDGF-BB–stimulated pericytes gained FSP1 expression, a fibroblast-specific marker, indicating that pericytes underwent a PFT transition (Fig. 2 *A* and *B*). The loss of expression of NG2 and gain of expression of FSP1 were further validated by Western immunoblot with specific antibodies (Fig. 2*C*).

We used anti-PDGFRα and anti-PDGFRβ specific neutralizing antibodies to delineate the receptor signaling responsible for PDGF-BB–induced PFT (23, 30). PDGFRβ neutralizing antibody blocked the PDGF-BB–induced PFT, whereas the anti-PDGFRα specific antibody had virtually no effect (Fig. 2*D*). Similarly, imatinib also effectively inhibited the PDGF-BB–induced PFT in this in vitro experiment setting. Both anti-PDGFRβ and imatinib prevented the loss of NG2 in pericytes

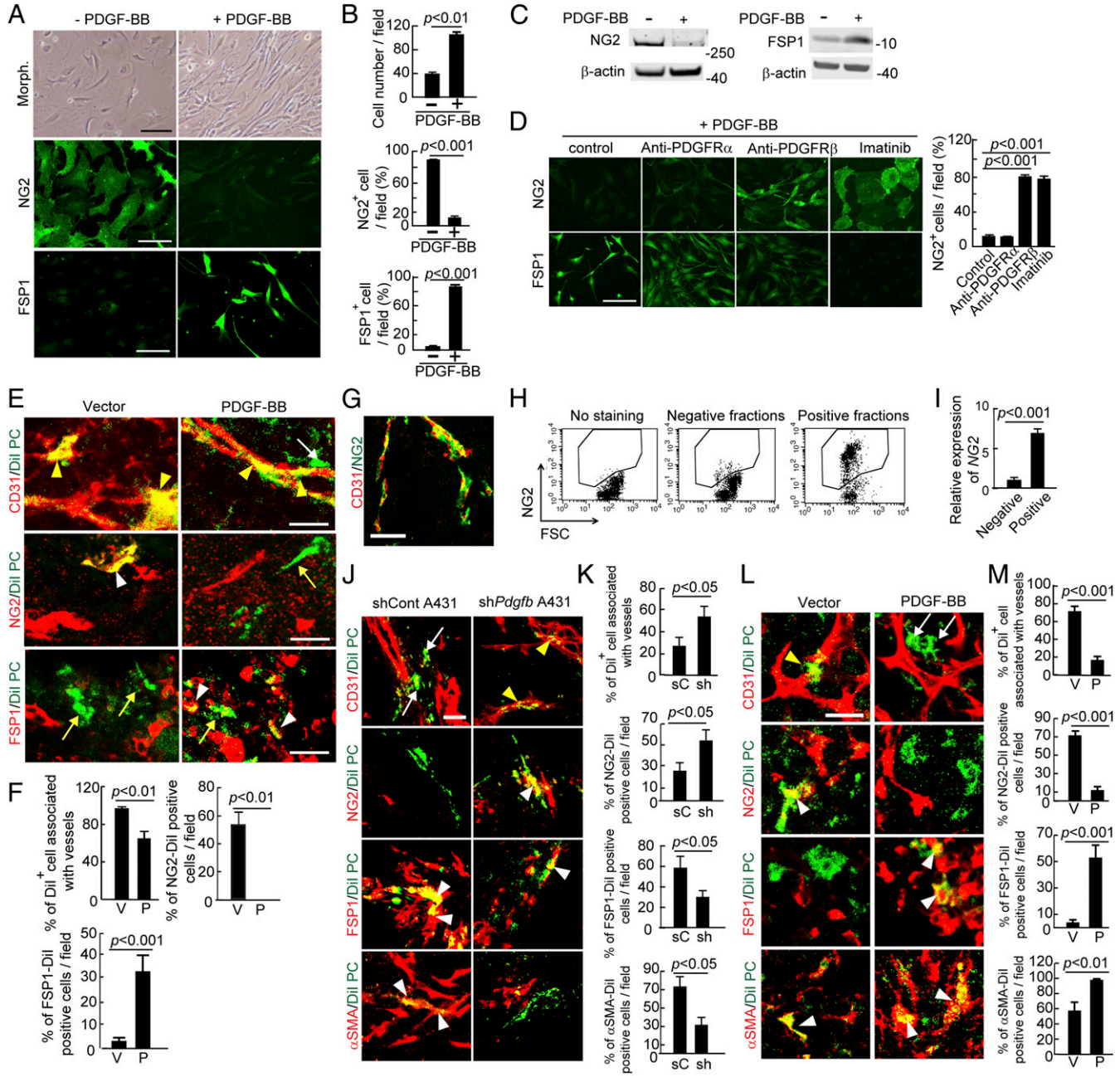

Fig. 2. PDGF-BB induces PFT in vivo and in vitro. (*A*) Morphology, NG2 positivity, and FSP1 positivity in PDGF-BB–stimulated and nonstimulated primary pericytes. (Scale bar, 100 μm.) (*B*) Quantification of cell proliferation, $NG2^+$ signals, and $FSP1^+$ signals ($n = 8$ fields per group). The experiments were repeated three times. (*C*) Western blot analysis of NG2 and FSP1 proteins in PDGF-BB–stimulated and nonstimulated primary pericytes. β-actin detection indicates the standard loading in each lane. (*D*) $NG2^+$ signals and $FSP1^+$ signals in buffer-, anti-PDGFRα-, anti-PDGFRβ-, and imatinib-treated pericytes that were stimulated with PDGF-BB. Quantification of $NG2^+$ cells in various treated groups ($n = 8$ fields per group). The experiments were repeated two times. (Scale bar, 100 μm.) (*E*) DiI-labeled pericytes (green) were implanted into T241-vector and T241-PDGF-BB tumors. Tumor vessels were stained with CD31 (red in *Top*), pericytes were stained with NG2 (red in *Middle*), and fibroblasts were stained with FSP1 (red in *Bottom*). Yellow arrowheads indicate vessel-associated DiI-labeled pericytes. White arrows indicate vessel-disassociated injected pericytes. The white arrowhead in the middle panel points to NG2 and DiI double signals and the yellow arrow in the middle panel indicates $NG2^-$ DiI^+ cells. Yellow arrows in the lower panels indicate $FSP1^-$ DiI^+ cells and white arrowheads in the lower panels point to $FSP1^+$ DiI^+ cells. (Scale bars, 25 μm.) (*F*) Quantification of $CD31^+$ vessel-associated DiI^+pericytes, $NG2^+DiI^+$ structures, and $FSP1^+DiI^+$ structures ($n = 12$ fields per group). Data are represented as mean ± SEM. P, PDGF-BB; V, vector. (*G*) Double immunohistochemical staining of human cancer tissue with CD31 (red) and NG2 (green). (Scale bar, 50 μm.) (*H*) FACS analysis of isolated $NG2^+$ human pericytes from human tumors. (*I*) Quantification of NG2 positive signals of isolated human pericytes by quantitative PCR (triplicates per sample). (*J*) Tracing DiI-labeled human pericytes (green) implanted in scrambled shRNA- and shPdgfb-transfected human A431 tumors. White arrows indicate vessel-disassociated pericytes, yellow arrowheads point to vessel associated pericytes, and white arrowheads indicate double positive signals. (Scale bar, 25 μm.) (*K*) Quantification of $CD31^+$vessel-associated DiI^+pericytes, $NG2^+DiI^+$ structures, $FSP1^+DiI^+$ structures, and αSMA^+DiI^+ structures ($n = 10$ fields per group). Data are represented as mean ± SEM. sC, scrambled control tumor; sh, shPdgfb-transfected tumor. (*L*) Tracing DiI-labeled human pericytes (green) implanted in vector- and PDGF-BB-LLC tumors. The yellow arrowhead points to vasculature-associated pericytes, and white arrows indicate vasculature-disassociated pericytes. White arrowheads indicate double positive signals. (Scale bar, 25 μm.) (*M*) Quantification of $CD31^+$vessel-associated DiI^+pericytes, $NG2^+DiI^+$ structures, $FSP1^+DiI^+$ structures, and αSMA^+DiI^+ structures ($n = 10$ fields per group). Data are represented as mean ± SEM. P, PDGF-BB; V, vector.

(Fig. 2*D*). These data show that PDGF-BB is capable of inducing PFT in isolated pericytes.

To further study whether PDGF-BB was able to induce PFT in in vivo tumors, isolated pericytes were labeled with DiI dye and injected into PDGF-BB and vector tumors. Consistent with in vitro findings, $NG2^+$ pericytes lost NG2 expression in PDGF-BB fibrosarcomas and gained FSP1 expression (Fig. 2 *E* and *F*). Similar results were also obtained from an independent PDGF-BB–expressing tumor, LLC-PDGF-BB (Fig. S6 *C* and *D*). Thus, PDGF-BB–induced PFT occurs in tumors in vivo.

Primary Pericytes Isolated from Human Tumors Undergo PFT in in Vivo Tumors. To link our findings to clinical relevance, we isolated primary pericytes from fresh human tumors using NG2 as a specific marker (Fig. 2 *G–I*). The isolated human pericytes were labeled with DiI dye and injected into naturally occurring human squamous carcinomas implanted in immunodeficient SCID mice. Injection of human pericytes into control shRNA-A431 human squamous carcinoma resulted in disassociation of pericytes from tumor vasculatures and gain of FSP1 and αSMA expression (Fig. 2 *J* and *K*). However, knockdown of PDGF-BB by a *shPdgfb* markedly inhibited PFT and the remaining pericytes were associated with tumor vessels (Fig. 2 *J* and *K*). To further validate these findings in human tumors, DiI-labeled isolated human pericytes were also injected into mouse tumors. Similar to human tumors, PDGF-BB disassociated pericytes from tumor vasculatures and stimulated PFT by gaining FSP1 and αSMA expression and loss of NG2 expression (Fig. 2 *L* and *M*). Taken together, these findings show that pericytes isolated from human tumor tissues are capable of PFT in human and mouse tumors. Thus, it is highly plausible that PFT also occurs in human tumors.

Genome-Wide Profiling Defines Fibroblast-Like Signatures of PDGF-BB–Stimulated Pericytes. To further define fibroblast signatures in PDGF-BB–stimulated pericytes, we performed genome-wide gene expression profiling and revealed marked changes of clusters of genes in PDGF-BB–stimulated and nonstimulated pericytes (Fig. 3*A*). A multiclass rank product analysis identified differentially expressed genes. Gene set enrichment analysis showed that proliferation was strongly induced early at day 1 but was later decreased at day 5 after PDGF-BB stimulation (Fig. 3*B*). A gene set representing epithelial-to-mesenchymal transition was enriched among up-regulated genes both after day-1 and day-5 stimulation with PDGF-BB (Fig. 3*B*). A heat map of known marker genes for pericytes, fibroblasts, and mesenchymal cells showed that PDGF-BB treatment of primary pericytes induced differentiation toward a fibroblast fate (Fig. 3*C*). Further analysis of stromal or mesenchymal cell-related genes using the random variance model supported the PDGF-BB–stimulated PFT (Fig. 3*D*). Further, we used a known mesenchymal fibroblast cell (S17) as a positive control to profile the similarities of up- and down-related genes in PDGF-BB–stimulated pericytes. Strikingly, we found that 77% of up- and down-regulated genes were in agreement with the fibroblast signature (Fig. 3*E*). Taken together, the genome-wide gene expression analysis demonstrates that PDGF-BB–stimulated pericytes possess fibroblast features.

Genetic Tracing of PFT in Tumors with Two Independent Mouse Strains. To provide definite evidence to further support the PDGF-BB–induced PFT, we generated two tumor models using genetically modified mouse strains that allowed us to trace pericytes in the tumor microenvironment. In the first model (*TN-AP Cre ERT2:R26R-tdTomato*), pericytes were genetically labeled with

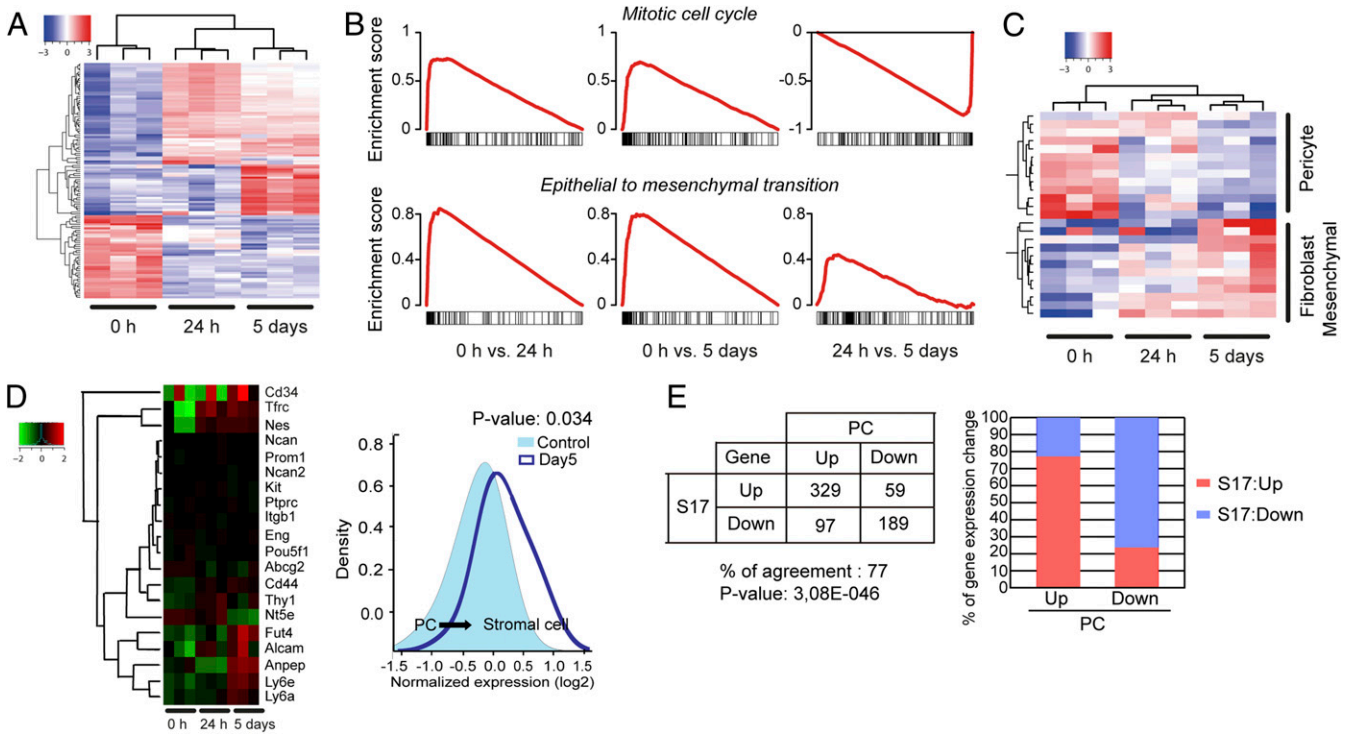

Fig. 3. Gene-expression profiling by genome-wide array analysis. (*A*) Differentially expressed genes (FDR < 0.05) at different time points as identified using a multiclass rank product analysis. (*B*) Gene set enrichment analysis shows that proliferation is strongly induced early after stimulation of pericytes with PDFGF-BB but decreased at day 5 in comparison with 24-h stimulation. A gene set representing epithelial-to-mesenchymal transition is enriched among up-regulated genes both after 24-h and 5-d stimulation with PDFG-BB. (*C*) A heat map of known marker genes for pericytes, fibroblasts, mesenchymal cells, and epithelial-to-mesenchymal transition, showing that PDFGF-BB treatment of primary pericytes induced differentiation toward a fibroblast fate. (*D*) Heat map of stromal and mesenchymal markers, supporting the PDGF-BB–induced differentiation from pericytes toward stromal fibroblasts. (*E*) Gene profiling similarities between known stromal fibroblasts (S17 mesenchymal fibroblasts) and PDGF-BB–stimulated pericytes (day 5).

Tomato Red as previously described (15). Both T241 vector and PDGF-BB–expressing tumors were implanted in *TN-AP Cre ERT2:R26R-tdTomato* mice. Expectedly, Texas Red tomato-labeled pericytes were mainly associated with tumor vasculatures in the vector tumors and a substantial number of Texas Red Tomato-labeled pericytes expressed NG2 marker (Fig. 4 *A* and *B*). In contrast, most Texas Red tomato-labeled pericytes lost NG2 expression and their association with tumor vasculatures in PDGF-BB tumors. Instead, these Texas Red tomato-labeled cells exhibited elongated morphologies typical of fibroblasts in appearance. Moreover, these labeled pericytes gained expression of FSP1 and PDGFRα, two commonly expressed cell surface markers in stromal fibroblasts (Fig. 4 *A* and *B*). These findings support the notion that genetically labeled pericytes in the tumor microenvironment undergo PFT in response to PDGF-BB stimulation.

To further validate these findings, we chose to use an independent mouse tracing strain in which specific expression of Texas Red Tomato was controlled by the NG2 Cre recombinase (*NG2 Cre ERT2:**R**26R-tdTomato*) (31). Again, in the vector tumor, most NG2 Texas Red Tomato-labeled pericytes were associated with tumor vessels and they retained their NG2 expression (Fig. 4 *C* and *D*). Strikingly, almost all NG2 Texas Red Tomato-labeled pericytes lost their NG2 expression and association with tumor vasculatures in PDGF-BB tumors, supporting our findings in nongenetically manipulated WT mice. In contrast, NG2 Texas Red Tomato-labeled pericytes significantly gained expression of FSP1 and PDGFRα (Fig. 4 *C* and *D*). These findings support PDGF-BB–triggered PFT in the tumor microenvironment.

PDGF-BB–Primed Pericytes Stimulate Tumor Growth and Metastasis. We next investigated functional impacts of PDGF-BB–stimulated pericytes in tumor growth and metastasis. Pericytes were stimulated with PDGF-BB–containing medium for 7 d and were subsequently coimplanted with EGFP-T241 tumor cells. Nonstimulated pericytes were used as controls. At day 24 after implantation, the PDGF-BB-pericytes+ tumor cell group grew significantly faster compared with the vehicle pericytes+ tumor cell group, indicating that PDGF-BB–stimulated pericytes play a significant role in stimulating tumor growth (Fig. 5*A*). Histological examination showed that tumors with PDGF-BB–stimulated pericytes possessed a higher density of microvessels relative to control tumors (Fig. 5 *B* and *C*). However, percentages of pericyte coverage in both PDGF-BB-pericyte and vehicle-pericyte+ tumors were identical (Fig. 5 *B* and *C*), suggesting that in vitro stimulation of pericytes with PDGF-BB did not affect their association with angiogenic vessels. Conversely, FSP1$^+$ CAFs were markedly increased in PDGF-BB-pericyte tumors compared with control tumors (Fig. 5*D*), supporting the view that PDGF-BB–stimulated pericytes underwent PFT transition.

It is known that increases of CAFs and angiogenic phenotype are correlated with invasiveness and metastatic phenotypes of solid tumors (6). To study the impact of PDGF-BB–stimulated pericytes in promoting cancer metastasis, we measured the number of circulating tumor cells (CTCs) in PDGF-BB-pericytes– and vehicle-pericytes–containing tumor-bearing mice. Interestingly, a significantly higher number of CTCs were found in PDGF-BB-pericytes–containing tumor-bearing mice compared with vehicle-pericytes–containing tumor-bearing mice (Fig. 5*E*). These data suggest that PDGF-BB–stimulated pericytes promote tumor cell intravasation in the primary sites. Consistent with increases of CTCs, culturing blood from PDGF-BB-pericytes–containing tumor-bearing mice resulted in a significantly increased number of tumor colonies compared with control group (Fig. 5*F*). Taken together, these results show that PDGF-BB–stimulated pericytes facilitate primary tumor growth and cancer metastasis through the mechanisms of tumor angiogenesis and intravasation.

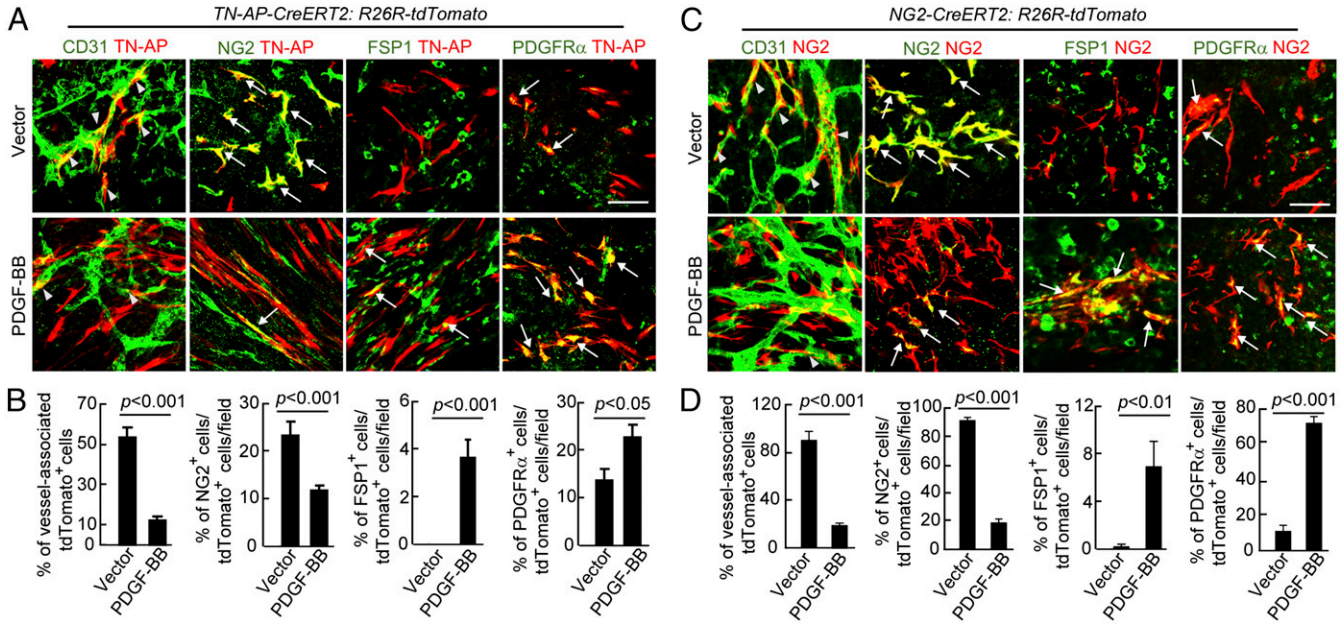

Fig. 4. Genetic tracing of pericytes in contribution to PFT. (*A*) Genetic tracing of differentiation of alkaline phosphatase (AP)-marked pericytes into fibroblasts in T241-vector and T241-PDGF-BB tumors. Tamoxifen-induced AP-tdTomato-red (red) tumor tissues were contained with CD31, NG2, FSP1, and PDGFRα. Yellow arrows indicate overlapping positive signals in each panel. Arrowheads point to vessel-associated AP-tdTomato+ pericytes. (Scale bar, 50 μm.) (*B*) Quantification of vessel-associated AP-tdTomato$^+$ cells, the total number of NG2$^+$ AP-tdTomato$^+$ structures, FSP1$^+$ AP-tdTomato$^+$ structures, and PDGFRα$^+$ AP-tdTomato$^+$ structures (n = 15 fields per group) in T241-vector and T241-PDGF-BB tumors. (*C*) Genetic tracing of differentiation of NG2-marked pericytes into fibroblasts in T241-vector and T241-PDGF-BB tumors. Tamoxifen-induced NG2-tdTomato-red (red) tumor tissues were contained with CD31, NG2, FSP1, and PDGFRα. Yellow arrows indicate overlapping positive signals in each panel. Arrowheads point to vessel-associated NG2-tdTomato$^+$ pericytes. (Scale bar, 50 μm.) (*D*) Quantification of vessel-associated NG2-tdTomato$^+$ cells, the total number of NG2$^+$ NG2-tdTomato$^+$ structures, FSP1$^+$ NG2-tdTomato$^+$ structures, and PDGFRα$^+$ NG2-tdTomato$^+$ structures (n = 15 fields per group) in T241-vector and T241-PDGF-BB tumors. Data are represented as mean ± SEM (n = 4 animals per group).

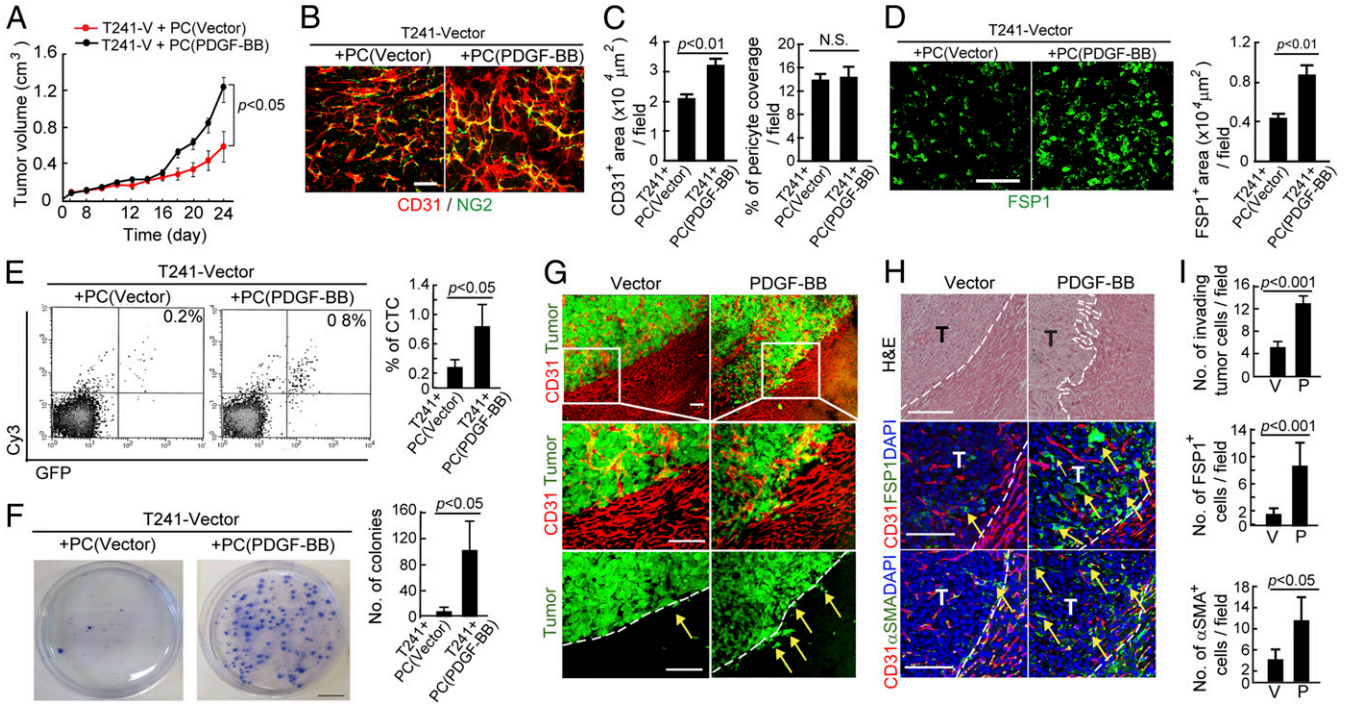

Fig. 5. PDGF-BB–stimulated pericytes promote tumor growth, angiogenesis, stromal fibroblast expansion, and metastasis. (*A*) Growth rates of nonstimulated pericyte-T241-vector cell- and PDGF-BB–stimulated pericyte-T241-vector-coimplanted primary tumors ($n = 8$ animals per group). (*B*) Microvessel density (CD31) and pericyte coverage (NG2) of nonstimulated pericyte-T241-vector cell- and PDGF-BB–stimulated pericyte-T241-vector-coimplanted primary tumors. (Scale bar, 50 μm.) (*C*) Quantification of $CD31^+$ vessel density and $NG2^+$ vascular pericyte coverage of nonstimulated pericyte-T241-vector cell- and PDGF-BB–stimulated pericyte-T241-vector-coimplanted primary tumors ($n = 7$ fields per group). N.S., not significant. (*D*) Immunostaining and quantification of $FSP1^+$ stromal fibroblasts of nonstimulated pericyte-T241-vector cell- and PDGF-BB–stimulated pericyte-T241-vector-coimplanted primary tumors ($n = 7$ fields per group). (Scale bar, 50 μm.) (*E*) FACS analysis of bloodstream CTCs of animals implanted with nonstimulated pericyte-T241-vector cell- and PDGF-BB–stimulated pericyte-T241-vector-coimplanted primary tumors. Right upper plots indicate CTCs and percent is shown on the plots. Quantification of percent of CTCs ($n = 7$ animals per group). (*F*) Tumor colony formation of peripheral blood from nonstimulated pericyte-T241-vector cell- and PDGF-BB–stimulated pericyte-T241-vector-coimplanted primary tumors ($n = 7$ animals per group). (Scale bar, 2 cm.) (*G*) Invasiveness of $EGFP^+$ T241-vector and T241-PDGF-BB tumors in relation to intra- and peritumoral microvessels ($CD31^+$). Dashed lines mark the tumor rims and arrows point to the invasive front. (Scale bar, 100 μm.) (*H*) $FSP1^+$ and αSMA^+ contents in relation to microvessels in the border regions of tumors. Dashed lines mark the tumor rims and arrows point to stromal fibroblasts or myofibroblasts. (Scale bar, 100 μm.) T, tumor. (*I*) Quantification of invasive tumor cells, numbers of $FSP1^+$ stromal fibroblasts, and numbers of αSMA^+ stromal myofibroblasts at the invasive fronts of tumors ($n = 10$ fields per group). Data are represented as mean ± SEM. P, PDGF-BB; V, vector.

Liver implantation of T241-PDGF-BB-EGFP and T241-vector-EGFP tumors allowed us to visualize the invasive front of tumor masses. T241-PDGF-BB tumors showed irregular fronts with invasive tumor cells compared with control tumors (Fig. 5 *G–I*). Importantly, numbers of $FSP1^+$ and αSMA^+ CAFs in PDGF-BB tumors were markedly increased in the invasive front of PDGF-BB tumors compared with those in control tumors (Fig. 5 *H* and *I*), suggesting that these CAFs, likely to be originated from pericytes, are involved in tumor invasion and metastasis. To further delineate the role of pericytes in tumor invasion, we coimplanted EGFP-T241 tumors with PDGF-BB– or vehicle-stimulated pericytes. Interestingly, coimplantation of PDGF-BB–stimulated pericytes with tumor cells resulted in an invasive phenotype and invasive scattered tumor cells could be detected in the tumor rims (Fig. 6 *A–C*). Again, high densities of $FSP1^+$ and αSMA^+ CAFs were accrued at the invasive leading front in tumors with PDGF-BB–stimulated pericytes compared with tumors containing vehicle-stimulated pericytes (Fig. 6 *A–C*). These data provide an independent line of evidence that PDGF-stimulated pericytes promote tumor invasiveness in the invasive tumor front.

Reverse Correlation of High *PDGFB* and *FSP1* Expression with Survival in Colorectal, Glioblastoma Multiforme, and Lung Cancer Patients. To relate our preclinical findings to clinical relevance, we performed metaanalyses of cancer patients to correlate *PDGFB* and *FSP1* expression levels to survival. Because cancer invasion and metastasis are the most common causes of cancer-related death, survival prognosis often reflects the invasive and metastatic situation of cancer patients. We chose three common cancers, including lung squamous cell carcinoma (LUSC), colorectal adenocarcinoma (COADREAD), and lower-grade glioma (LGG), for further analysis. In this clinical study, datasets of 391 LUSC, 72 COADREAD, and 212 LGG patients were included in our study. Numbers of *PDGFB*-low patients include 192 LUSC, 36 COADREAD, and 105 LGG, and *PDGFB*-high patients include 199 LUSC, 36 COADREAD, and 107 LGG. Markedly, *PDGFB*-high groups in all three cancer types showed significantly shortened survivals compared with their corresponding *PDGFB*-low groups (Fig. 6 *D–F*).

We next correlated *PDGFB*-high and -low groups with the *FSP1* expression levels in these tumors. Strikingly, $FSP1^+$ fibrotic contents were significantly higher in *PDGFB*-high groups compared with *PDGFB*-low groups of these cancer patients (Fig. 6 *G–I*). The results from three cohort analyses provide clinical evidence of reverse correlation between *PDGFB* and *FSP1* expression with survival. Based on these clinical findings, it is reasonable to speculate that *PDGFB* and *FSP1* could potentially serve as prognostic markers to predict survivals of LUSC, COADREAD, and LGG patients.

Discussion

CAFs are one of the major host cellular components in many solid tumors, and infiltration of this stromal component has been

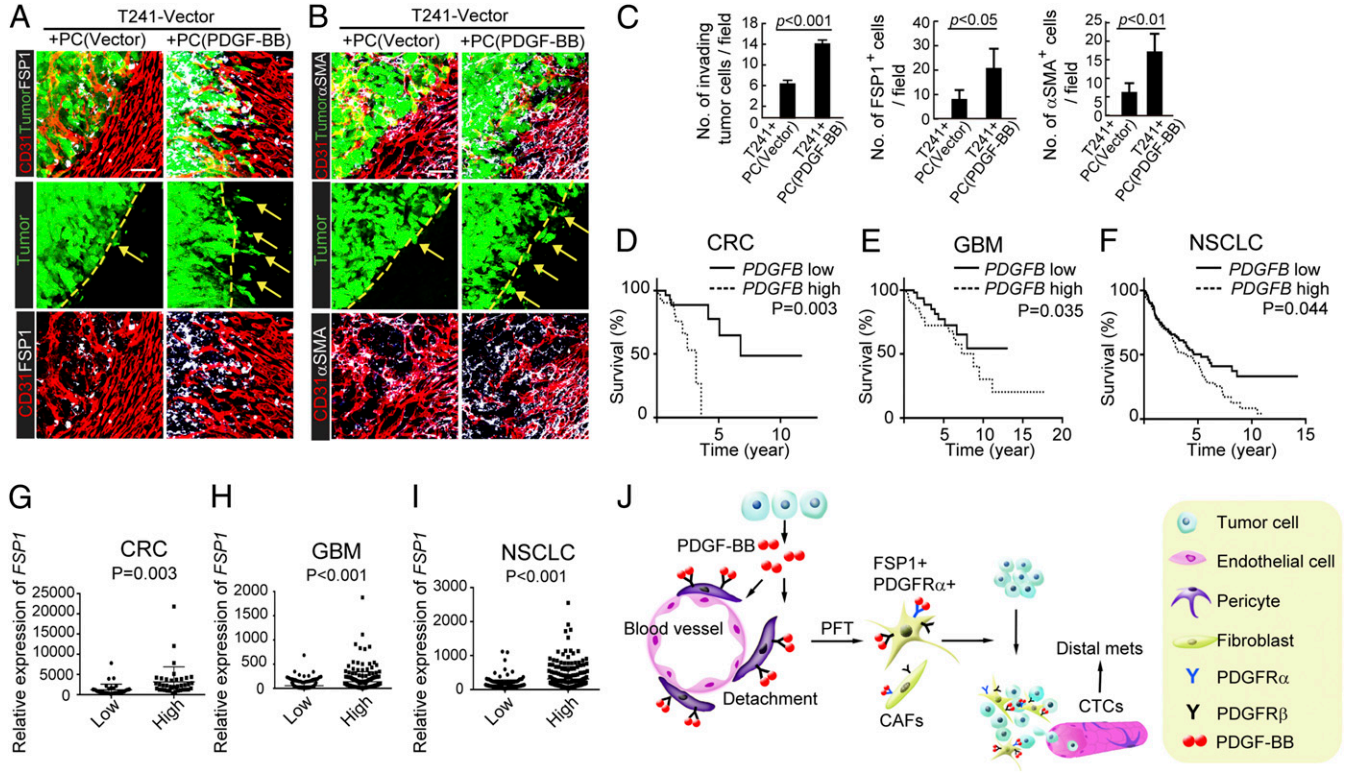

Fig. 6. PDGF-BB–stimulated pericytes promote primary cancer invasiveness. (*A*) Invasiveness of nonstimulated pericyte- EGFP$^+$ T241-vector cell- and PDGF-BB–stimulated pericyte- EGFP$^+$ T241-vector-coimplanted primary tumors in relation to FSP1$^+$ stromal fibroblasts (white) and CD31+ intra- and peritumoral microvessels (red). Dashed lines mark the tumor rims and arrows point to the invasive front. $n = 8$ animals per group. (Scale bar, 50 μm.) (*B*) Invasiveness of nonstimulated pericyte- EGFP$^+$ T241-vector cell- and PDGF-BB–stimulated pericyte- EGFP$^+$ T241-vector-coimplanted primary tumors in relation to αSMA$^+$ (white) stromal myofibroblasts and CD31+ intra- and peritumoral microvessels (red). Dashed lines mark the tumor rims and arrows point to the invasive front. $n = 8$ animals per group. (Scale bar, 50 μm.) (*C*) Quantification of invasive tumor cells, numbers of FSP1$^+$ stromal fibroblasts, and numbers of αSMA$^+$ stromal myofibroblasts at the invasive fronts of nonstimulated pericyte-T241-vector cell- and PDGF-BB–stimulated pericyte-T241-vector-coimplanted primary tumors ($n = 10$ fields per group). (*D*) Kaplan–Meier survival of *PDGFB*-high ($n = 36$) and *PDGFB*-low ($n = 36$) COADREAD patients. (*E*) Kaplan–Meier survival of *PDGFB*-high ($n = 107$) and *PDGFB*-low ($n = 105$) LGG patients. (*F*) Kaplan–Meier survival of *PDGFB*-high ($n = 199$) and *PDGFB*-low ($n = 192$) LUSC patients. (*G*) Correlation of FSP1 expression in *PDGFB*-high ($n = 36$) and *PDGFB*-low ($n = 36$) COADREAD patients. (*H*) Correlation of FSP1 expression in PDGF-BB-high ($n = 107$) and PDGF-BB-low ($n = 105$) LGG patients. (*I*) Correlation of FSP1 expression in *PDGFB*-high ($n = 199$) and *PDGFB*-low ($n = 192$) LUSC patients. (*J*) Diagram of tumor-derived PDGF-BB in promoting tumor invasion and metastasis. Tumor cell-derived PDGF-BB builds up a high gradient that attracts pericytes to move away from tumor microvessels. Once pericytes detach, they differentiate into stromal fibroblast (PFT) in the presence of PDGF-BB. Increases of stromal fibroblasts and myofibroblasts in tumors significantly promote tumor cell invasion and intravasation into the circulation, leading to an increase of CTCs and distal metastasis. Data are represented as mean ± SEM.

correlated with invasiveness and poor prognosis of cancer disease (5, 6). In this study, we address an important issue related to the origin of CAFs in the tumor microenvironment. We have revealed a mechanism by which perivascular cells serve as a reservoir for stromal fibroblasts and the PFT is controlled by tumor-derived factors. Our study provides another example of how tumor cells manipulate the host-cell interaction for their growth and invasion. Although genetic mutations in malignant cells are important for tumor growth and invasion, the microenvironment composed of host cells is a crucial element that determines the invasive phenotype of tumor cells. To metastasize to distal organs, malignant cells at the primary site have to interact with host cells, including inflammatory cells, fibroblasts, and vascular cells, to intravasate into the circulation (32, 33). Intravasation, one of the initial steps of the metastatic cascade, is a complex process that requires several cell types to interact and transmigrate through the vascular endothelium in a cooperative manner. Several key issues related to tumor cell invasion and the underlying molecular mechanism remain unclear. How is this multicellular process modulated in the tumor microenvironment? What are the origins of CAFs? What are the functions of perivascular cells in cancer metastasis? How are these host cells positioned at the invasive fronts? What are the signaling molecules and pathways that control tumor invasion?

Whereas most host-cell types in the tumor microenvironment, including inflammatory cells, endothelial cells, and stromal fibroblasts, are well-characterized, the biological functions of pericytes in association with cancer metastasis remain largely unknown. Would high numbers of pericytes be advantageous for tumor growth and metastasis? If so, would associated or diassociated pericytes facilitate tumor growth and metastasis? In tumors, pericytes are widely believed to play a role in the recruitment of pericytes onto angiogenic vessels, leading to vascular remodeling toward a maturation phenotype (12, 16). PDGF-BB is one of the key factors involved in pericyte migration and association with angiogenic vessels. Disruption of pericyte coverage in tumor angiogenic vessels would likely increase the tortuosity and disorganization of tumor vessels, resulting in an accelerated tumor growth rate (34). In support of this view, ablation of pericytes by anti-PDGF agents has been reported to increase vascular tortuosity and tumor growth, suggesting that vascular recruitment of pericytes by PDGF-BB plays a negative role in tumor angiogenesis and growth (35, 36). Paradoxically, inhibition of PDGF-BB–mediated pericyte association to tumor vessels has also been reported to be a valid target for cancer

therapy, particularly when targeted in combination with other angiogenic factors (35, 37–39). For example, combining anti-VEGF and anti-PDGF drugs provides an additive therapeutic effect (40). One explanation of the combination approach is that anti-PDGF drugs increase exposure of vascular endothelial cells to anti-VEGF agents by ablating perivascular cells. Despite these claims of vasculature-related functions, the action of pericytes per se on modulation of the tumor microenvironment, tumor growth, and metastasis are poorly understood. In particular, molecular players controlling pericyte differentiation in tumors remain unidentified.

We are beginning to understand the complex role of pericytes in modulation of cancer metastasis. Our recent work and work published by others shows that loss of pericytes makes the tumor vessels more susceptible for cancer cell intravasation and eventually metastasis (23, 41). Apart from pericytes and malignant cancer cells, other cell types such as tumor-associated macrophages and cancer-associated fibroblasts are also involved in the intravasation cascade (6, 33). Loss of pericytes from tumor vessels may either permit tumor cell intravasation and PFT or hijack tumor cells for intravasation, and perhaps even the formation of the initial metastatic niches in distal tissues and organs. Indeed, it has been described that tumors can carry their own fibroblasts as "soil" for them to "seed" and grow in distal organs (42). Therefore, pericytes play dynamic roles in cancer invasion and metastasis.

In this study, we show that PDGF-BB plays dual roles in modulation of pericyte functions. First, tumor cell-derived PDGF-BB ablates pericytes from tumor microvessels. The possible mechanism underlying pericyte ablation is that the high PDGF-BB gradient from the tumor cell source attracts pericytes to move toward tumor cells rather than to endothelial cells (23). Second, once pericytes disassociate from tumor vasculatures, they undergo PFT under persistent PDGF-BB stimulation in the tumor microenvironment (Fig. 6*J*). These findings may imply that (*i*) pericytes have an intrinsic property that displays high potential capacity and plasticity of differentiating into other cell types, (*ii*) endothelial cells in the vessel wall might prevent differentiation of pericytes into other cell types and maintain pericyte stemness features, and (*iii*) under the influence of a specific signaling pathway pericytes may commit to differentiation toward a specific cell type. In our mouse and human tumor experimental models we demonstrate that the PDGF-BB-PDGFRβ signaling system drives pericyte differentiation toward fibroblasts. It is unclear whether the PDGF-BB-PDGFRβ signaling pathway either alone or in combination with other signaling pathways induces pericyte differentiation toward other lineages.

One of the surprising findings of our present work is that PDGF-BB–expressing tumors almost completely lack $NG2^+$ pericyte expression. Assuming that tumor cell-derived PDGF-BB ablates pericytes from tumor vessels, these $NG2^+$ pericytes would have remained as vessel-disassociated $NG2^+$ cells, which would still be detected. The loss of $NG2^+$ cells is neither due to down-regulation of this cell surface marker by PDGF-BB stimulation nor to increased cell death. Two genetic tracing mouse strains provide compelling and convincing evidence supporting PFT. Although it is known that PDGF-BB tumors contain high amounts of stromal components (30), their origins remain unclear. There are three possible mechanisms by which PDGF-BB contributes to the tumor stromal cell component: (*i*) induction of proliferation of existing fibroblasts for expansion, (*ii*) recruitment of fibroblasts from neighbor or distal tissues because PDGF-BB is a potent factor for cell migration, and (*iii*) differentiation of stem cells and other cell types into fibroblasts. Here, we demonstrate pericyte differentiation as a mechanism of increasing fibroblast components in PDGF-BB tumors. Our data could also be applicable in PDGF-BB negative tumors because PDGFRβ could be activated by alternative mechanisms. For example, other members in the PDGF family, including PDGF-DD and PDGF-CC, could also activate PDGFRβ (43–46). Moreover, genetic mutations of PDGFRβ could cause ligand-independent activation of this receptor (47). Also, high expression of PDGFRβ in pericytes and stromal cells might cause autophosphorylation of PDGFRβ, leading to the formation of receptor dimers, oligomers, and aggregates (48–50). These interesting possibilities warrant future validation.

Preclinical and clinical evidence shows that the tumor stroma is strongly correlated with an invasive and metastatic phenotype of most solid tumors (51–53). In a mouse experimental metastatic model in our previous study we showed that PDGF-BB–producing tumor cells readily form clusters and are colonized in distal tissues and organs such as the lung (23). These findings are consistent with results by others demonstrating that stromal fibroblasts promote metastatic tumor growth via stimulation of tumor angiogenesis (37). Moreover, in the tumor environment, angiogenic vessels would facilitate pericyte infiltrations, which would subsequently undergo PFT by PDGF-BB. CAFs are crucial for the formation of tumor niches, and they often serve as feeder cells that support malignant cell adhesion, expansion, and invasion. Thus, tumor-derived PDGF-BB contributes to the metastatic cascade by facilitating multiple steps including stimulation of dissemination, recolonization, and regrowth. Our findings from animal tumor models are highly relevant to clinical settings in which human tumors produce high levels of PDGF-BB. Similar to genetically engineered mouse tumors, we provide evidence that human PDGF-BB–producing tumors in their intrinsic status exhibit pericyte ablation and disassociation from tumor vessels. Conversely, we demonstrate substantial expansion of the stromal compartment in PDGF-BB–positive tumors compared with PDGF-BB–negative tumors. Thus, these findings recapitulate the clinical situation in cancer patients. A rational speculation of our work is that PDGF-BB might serve as an important biomarker for predicting tumor invasion, metastasis, and drug resistance.

Our clinical data support the fact that high *PDGFB* expression in human cancers is reversely correlated with survival prognosis. In three cohort analyses of LUSC, COADREAD and LGG we show that high *PDGFB* levels serve as an independent prognostic marker for poor survival. Moreover, high *PDGFB* expression is positively correlated to the high content of stromal fibroblasts in tumors. Although tracing the fate of pericytes in human patients remains as a challenging issue because it cannot be performed, it is highly plausible that PDGF-BB is the driving force for expansion of CAFs in these cancer patients as well. In support of this notion, we demonstrate that pericytes isolated from human tumors are capable of undergoing PFT in human tumors. Because cancer metastasis is a common reason for cancer death, the reduced survival time of *PDGFB*-high and *FSP1*-high patients is likely due to cancer invasion and metastasis.

Taken together, our data provide evidence of cell-type switching in the tumor microenvironment and define functions of pericytes in cancer invasion and metastasis. Targeting the PDGF-BB-PDGFRβ–induced PFT would be an important therapeutic approach for the treatment of cancer and metastasis.

Materials and Methods

Animals. Male and female C57/B6 mice at age 4 to 6 wk were used for xenograft tumor studies. Male or female SCID mice, *Pdgfrβ*$^{-/-}$ mice, *TN-AP Cre ERT2:R26R-tdTomato* mice, and *NG2 Cre ERT2:R26R-tdTomato* mice at age 4 to 8 wk were used as knockout and transgenic mouse strains. All mouse studies were approved by the Northern Stockholm Experimental Animal Ethical Committee. See *SI Materials and Methods* for more details.

Human Samples. Human tissues materials were obtained from the Karolinska Hospital and the procedure of human sample handling and informed consent were followed according to the regulation approved by the Karolinska Biobank Review Board (permission no. BbK1228). Accordingly, all patient materials were anonymized before being transferred to research laboratories. Isolated cells from fresh human samples were injected into mice immediately without cultivation.

Cell Lines and Culture. T241, LLC, A431, and CAKI-1 tumor cell lines were cultured in DMEM. The IMR32 tumor cell line was maintained in RPMI1640 medium. Mouse

primary PCs were maintained in DMEM. See *SI Materials and Methods* for details and also for details on *Pdgfb*-shRNA knockdown, whole-mount staining, immunohistochemical staining, isolation of primary pericytes from fresh human tumor tissues, measurement of CTC, ELISA, quantitative real-time and RT-PCR, immunoblotting, and correlation of *PDGFB* expression in human cancer patients.

Affymetrix Gene-Array Analysis. Data have been deposited in the Gene Expression Omnibus with accession nos. GSE85955 and GSE33717 (30). See *SI Materials and Methods* for details.

Statistical Analysis. Statistical analyses of results except gene array analysis were performed using the standard two-tailed Student t test, and $P < 0.05$ was considered statistically significant.

ACKNOWLEDGMENTS. We thank Funeng Jiang, Xiaojuan Yang, Yin Zhang, and Hideki Iwamoto for technical assistance; and Dr. Funa Keiko (Gothenburg University) and Dr. Xuri Li (Zhongshan Ophthalmology Center, Sun Yat-sen University) for providing tumor cell lines. Y.C.'s laboratory is supported through research grants from the Swedish Research Council, the Swedish Cancer Foundation, the Karolinska Institute Foundation, a Karolinska Institute distinguished professor award, the Torsten Soderbergs Foundation, the Tore Nilsons Foundation, the Ruth and Richard Julin Foundation, the Ogonfonden Foundation, the Martin Rinds Foundation, the Maud and Birger Gustavssons Foundation, the Lars Hiertas Minne Foundation, the Alex and Eva Wallströms Foundation, the Robert Lundbergs Memorial Foundation, the Swedish Diabetes Foundation, the Swedish Children Cancer Foundation, European Research Council Advanced Grant ANGIOFAT (Project 250021), the Knut Alice Wallenberg Foundation, and an advanced grant from NOVO Nordisk Foundation.

1. Hanahan D, Weinberg RA (2011) Hallmarks of cancer: The next generation. *Cell* 144(5):646–674.
2. Cao Y, et al. (2011) Forty-year journey of angiogenesis translational research. *Sci Transl Med* 3(114):114rv3.
3. Ferrara N, Kerbel RS (2005) Angiogenesis as a therapeutic target. *Nature* 438(7070):967–974.
4. Grivennikov SI, Greten FR, Karin M (2010) Immunity, inflammation, and cancer. *Cell* 140(6):883–899.
5. Mueller MM, Fusenig NE (2004) Friends or foes—Bipolar effects of the tumour stroma in cancer. *Nat Rev Cancer* 4(11):839–849.
6. Kalluri R, Zeisberg M (2006) Fibroblasts in cancer. *Nat Rev Cancer* 6(5):392–401.
7. Folkman J (2007) Angiogenesis: An organizing principle for drug discovery? *Nat Rev Drug Discov* 6(4):273–286.
8. Lim SD, et al. (2007) Expression of the neural stem cell markers NG2 and L1 in human angiomyolipoma: Are angiomyolipomas neoplasms of stem cells? *Mol Med* 13(3-4):160–165.
9. Govindarajan B, et al. (2012) Cooperative benefit for the combination of rapamycin and imatinib in tuberous sclerosis complex neoplasia. *Vasc Cell* 4(1):11.
10. Pillai VB, et al. (2015) Honokiol blocks and reverses cardiac hypertrophy in mice by activating mitochondrial Sirt3. *Nat Commun* 6:6656.
11. Armulik A, Genové G, Betsholtz C (2011) Pericytes: Developmental, physiological, and pathological perspectives, problems, and promises. *Dev Cell* 21(2):193–215.
12. von Tell D, Armulik A, Betsholtz C (2006) Pericytes and vascular stability. *Exp Cell Res* 312(5):623–629.
13. Crosby JR, Seifert RA, Soriano P, Bowen-Pope DF (1998) Chimaeric analysis reveals role of Pdgf receptors in all muscle lineages. *Nat Genet* 18(4):385–388.
14. Cao Y (2013) Angiogenesis and vascular functions in modulation of obesity, adipose metabolism, and insulin sensitivity. *Cell Metab* 18(4):478–489.
15. Dellavalle A, et al. (2011) Pericytes resident in postnatal skeletal muscle differentiate into muscle fibres and generate satellite cells. *Nat Commun* 2:499.
16. Hirschi KK, D'Amore PA (1996) Pericytes in the microvasculature. *Cardiovasc Res* 32(4):687–698.
17. Mills SJ, Cowin AJ, Kaur P (2013) Pericytes, mesenchymal stem cells and the wound healing process. *Cells* 2(3):621–634.
18. Tian X, et al. (2014) Vessel formation. De novo formation of a distinct coronary vascular population in neonatal heart. *Science* 345(6192):90–94.
19. Chen YT, et al. (2011) Platelet-derived growth factor receptor signaling activates pericyte-myofibroblast transition in obstructive and post-ischemic kidney fibrosis. *Kidney Int* 80(11):1170–1181.
20. Humphreys BD, et al. (2010) Fate tracing reveals the pericyte and not epithelial origin of myofibroblasts in kidney fibrosis. *Am J Pathol* 176(1):85–97.
21. Betsholtz C (1995) Role of platelet-derived growth factors in mouse development. *Int J Dev Biol* 39(5):817–825.
22. Lindahl P, Johansson BR, Levéen P, Betsholtz C (1997) Pericyte loss and microaneurysm formation in PDGF-B-deficient mice. *Science* 277(5323):242–245.
23. Hosaka K, et al. (2013) Tumour PDGF-BB expression levels determine dual effects of anti-PDGF drugs on vascular remodelling and metastasis. *Nat Commun* 4:2129.
24. Bardeesy N, DePinho RA (2002) Pancreatic cancer biology and genetics. *Nat Rev Cancer* 2(12):897–909.
25. Heinrich MC, Blanke CD, Druker BJ, Corless CL (2002) Inhibition of KIT tyrosine kinase activity: A novel molecular approach to the treatment of KIT-positive malignancies. *J Clin Oncol* 20(6):1692–1703.
26. Savage DG, Antman KH (2002) Imatinib mesylate—A new oral targeted therapy. *N Engl J Med* 346(9):683–693.
27. Shah NP, Sawyers CL (2001) Recent success with the tyrosine kinase inhibitor STI-571—Lessons for targeted therapy of cancer. *Curr Opin Investig Drugs* 2(3):422–423.
28. Sawyers CL (2002) Disabling Abl-perspectives on Abl kinase regulation and cancer therapeutics. *Cancer Cell* 1(1):13–15.
29. Gao Z, et al. (2005) Deletion of the PDGFR-beta gene affects key fibroblast functions important for wound healing. *J Biol Chem* 280(10):9375–9389.
30. Xue Y, et al. (2011) PDGF-BB modulates hematopoiesis and tumor angiogenesis by inducing erythropoietin production in stromal cells. *Nat Med* 18(1):100–110.
31. Kramann R, Humphreys BD (2014) Kidney pericytes: Roles in regeneration and fibrosis. *Semin Nephrol* 34(4):374–383.
32. Joyce JA, Pollard JW (2009) Microenvironmental regulation of metastasis. *Nat Rev Cancer* 9(4):239–252.
33. Pollard JW (2004) Tumour-educated macrophages promote tumour progression and metastasis. *Nat Rev Cancer* 4(1):71–78.
34. McCarty MF, et al. (2007) Overexpression of PDGF-BB decreases colorectal and pancreatic cancer growth by increasing tumor pericyte content. *J Clin Invest* 117(8):2114–2122.
35. Furuhashi M, et al. (2004) Platelet-derived growth factor production by B16 melanoma cells leads to increased pericyte abundance in tumors and an associated increase in tumor growth rate. *Cancer Res* 64(8):2725–2733.
36. Pietras K, Sjöblom T, Rubin K, Heldin CH, Ostman A (2003) PDGF receptors as cancer drug targets. *Cancer Cell* 3(5):439–443.
37. Crawford Y, et al. (2009) PDGF-C mediates the angiogenic and tumorigenic properties of fibroblasts associated with tumors refractory to anti-VEGF treatment. *Cancer Cell* 15(1):21–34.
38. Greenberg JI, et al. (2008) A role for VEGF as a negative regulator of pericyte function and vessel maturation. *Nature* 456(7223):809–813.
39. Pietras K, Pahler J, Bergers G, Hanahan D (2008) Functions of paracrine PDGF signaling in the proangiogenic tumor stroma revealed by pharmacological targeting. *PLoS Med* 5(1):e19.
40. Kuhnert F, et al. (2008) Soluble receptor-mediated selective inhibition of VEGFR and PDGFRbeta signaling during physiologic and tumor angiogenesis. *Proc Natl Acad Sci USA* 105(29):10185–10190.
41. Xian X, et al. (2006) Pericytes limit tumor cell metastasis. *J Clin Invest* 116(3):642–651.
42. Duda DG, et al. (2010) Malignant cells facilitate lung metastasis by bringing their own soil. *Proc Natl Acad Sci USA* 107(50):21677–21682.
43. Bergsten E, et al. (2001) PDGF-D is a specific, protease-activated ligand for the PDGF beta-receptor. *Nat Cell Biol* 3(5):512–516.
44. Cao R, et al. (2002) Angiogenesis stimulated by PDGF-CC, a novel member in the PDGF family, involves activation of PDGFR-alphaalpha and -alphabeta receptors. *FASEB J* 16(12):1575–1583.
45. LaRochelle WJ, et al. (2001) PDGF-D, a new protease-activated growth factor. *Nat Cell Biol* 3(5):517–521.
46. Li X, et al. (2000) PDGF-C is a new protease-activated ligand for the PDGF alpha-receptor. *Nat Cell Biol* 2(5):302–309.
47. Heinrich MC, et al. (2003) PDGFRA activating mutations in gastrointestinal stromal tumors. *Science* 299(5607):708–710.
48. Drummond-Barbosa DA, Vaillancourt RR, Kazlauskas A, DiMaio D (1995) Ligand-independent activation of the platelet-derived growth factor beta receptor: Requirements for bovine papillomavirus E5-induced mitogenic signaling. *Mol Cell Biol* 15(5):2570–2581.
49. Herrlich A, et al. (1998) Ligand-independent activation of platelet-derived growth factor receptor is a necessary intermediate in lysophosphatidic, acid-stimulated mitogenic activity in L cells. *Proc Natl Acad Sci USA* 95(15):8985–8990.
50. Lai CC, Henningson C, DiMaio D (1998) Bovine papillomavirus E5 protein induces oligomerization and trans-phosphorylation of the platelet-derived growth factor beta receptor. *Proc Natl Acad Sci USA* 95(26):15241–15246.
51. Karnoub AE, et al. (2007) Mesenchymal stem cells within tumour stroma promote breast cancer metastasis. *Nature* 449(7162):557–563.
52. Liotta LA, Kohn EC (2001) The microenvironment of the tumour-host interface. *Nature* 411(6835):375–379.
53. Thiery JP, Acloque H, Huang RY, Nieto MA (2009) Epithelial-mesenchymal transitions in development and disease. *Cell* 139(5):871–890.
54. Dong M, et al. (2013) Cold exposure promotes atherosclerotic plaque growth and instability via UCP1-dependent lipolysis. *Cell Metab* 18(1):118–129.
55. Hedlund EM, et al. (2013) Tumor cell-derived placental growth factor sensitizes antiangiogenic and antitumor effects of anti-VEGF drugs. *Proc Natl Acad Sci USA* 110(2):654–659.
56. Nissen LJ, et al. (2007) Angiogenic factors FGF2 and PDGF-BB synergistically promote murine tumor neovascularization and metastasis. *J Clin Invest* 117(10):2766–2777.
57. Yang X, et al. (2013) Vascular endothelial growth factor-dependent spatiotemporal dual roles of placental growth factor in modulation of angiogenesis and tumor growth. *Proc Natl Acad Sci USA* 110(34):13932–13937.
58. Yang Y, et al. (2013) Anti-VEGF- and anti-VEGF receptor-induced vascular alteration in mouse healthy tissues. *Proc Natl Acad Sci USA* 110(29):12018–12023.
59. Cao R, et al. (2004) PDGF-BB induces intratumoral lymphangiogenesis and promotes lymphatic metastasis. *Cancer Cell* 6(4):333–345.
60. Cao R, et al. (2012) Collaborative interplay between FGF-2 and VEGF-C promotes lymphangiogenesis and metastasis. *Proc Natl Acad Sci USA* 109(39):15894–15899.
61. Dai M, et al. (2005) Evolving gene/transcript definitions significantly alter the interpretation of GeneChip data. *Nucleic Acids Res* 33(20):e175.
62. Wright GW, Simon RM (2003) A random variance model for detection of differential gene expression in small microarray experiments. *Bioinformatics* 19(18):2448–2455.